

**This is a self-archived version of an original article. This version may differ from the original in pagination and typographic details.**

**Author(s):** Chrysalidis, K.; Wilkins, S. G.; Heinke, R.; Koszorus, A.; de Groote, Ruben; Fedosseev, V. N.; Marsh, B.; Rothe, S.; Ruiz, R. Garcia; Studer, D.; Vernon, A.; Wendt, K.

**Title:** First demonstration of Doppler-free 2-photon in-source laser spectroscopy at the ISOLDE-RILIS

**Year:** 2020

**Version:** Accepted version (Final draft)

**Copyright:** © 2019 Elsevier B.V. All rights reserved.

**Rights:** CC BY-NC-ND 4.0

**Rights url:** <https://creativecommons.org/licenses/by-nc-nd/4.0/>

**Please cite the original version:**

Chrysalidis, K., Wilkins, S. G., Heinke, R., Koszorus, A., de Groote, R., Fedosseev, V. N., Marsh, B., Rothe, S., Ruiz, R. G., Studer, D., Vernon, A., & Wendt, K. (2020). First demonstration of Doppler-free 2-photon in-source laser spectroscopy at the ISOLDE-RILIS. *Nuclear Instruments and Methods in Physics Research. Section B: Beam Interactions with Materials and Atoms*, 463, 476-481. <https://doi.org/10.1016/j.nimb.2019.04.020>

# First demonstration of Doppler-free 2-photon in-source laser spectroscopy at the ISOLDE-RILIS

K. Chrysalidis<sup>1,2,\*</sup>, S. G. Wilkins<sup>1</sup>, R. Heinke<sup>2</sup>, A. Koszorus<sup>3</sup>, R. De Groote<sup>4</sup>, V.N. Fedosseev<sup>1</sup>, B. Marsh<sup>1</sup>, S. Rothe<sup>1</sup>, R. Garcia Ruiz<sup>1</sup>, D. Studer<sup>2</sup>, A. Vernon<sup>5</sup>, K. Wendt<sup>2</sup>

## Abstract

Collinear Doppler-free 2-photon resonance ionization has been applied inside a hot cavity laser ion source environment at CERN-ISOLDE. An injection-seeded Ti:sapphire ring laser was used to generate light pulses with a Fourier-limited linewidth for high-resolution spectroscopy. Using a molybdenum foil as a reflective surface positioned at the end of the target transfer line, rubidium was successfully ionized inside the hot cavity. The results are presented alongside previously obtained data from measurements performed at the RISIKO mass separator at Mainz University, where collinear and perpendicular ionization geometries were tested inside an RFQ ion guide. This work is a pre-cursor to the application of the Doppler-free 2-photon in-source spectroscopy method at ISOLDE. This approach aims to take advantage of the unmatched sensitivity of in-source spectroscopy, without the disadvantage of Doppler broadening.

## 1. Introduction

The Resonance Ionization Laser Ion Source (RILIS) is by far the most commonly used ion source at the CERN-ISOLDE facility [1]. As it is based on the principle of stepwise resonant ionization, atomic properties of an element can be directly extracted from the energy information measured by the corresponding resonant transition, making it a valuable spectroscopic tool.

This so-called 'in-source resonance ionization spectroscopy' has been applied in numerous experimental campaigns, measuring the isotope shifts (IS) and hyperfine structure (HFS) of atomic transitions. Some of the most recent examples include investigations into the odd-even staggering effects in mercury [2], which was the first nuclear structure study using the newly-established RILIS-mode of the ISOLDE Versatile Arc Discharge (Laser) Ion Source (VAD(L)IS) [3].

The achievable resolution of the technique is limited by the Doppler broadening of the atomic spectral lines at the operating temperature of the ion source cavity ( $\sim 2000^\circ\text{C}$ ). For this reason, its application has been limited to the heavier elements (for which the Doppler broadening is reduced) and to atomic transitions that show high sensitivity to changes in the nuclear charge radius or nuclear moments (respectively, the IS or the HFS should be greater than the Doppler broadening).

Here we report on an approach to largely eliminate the Doppler broadening of the spectroscopic transition through the use of 2-photon transitions induced by co- and counter-propagating laser beams from the same laser source. The general theory of a 2-photon quantum transition was first described in the thesis of M. Göppert-Mayer in 1930 [4], whilst the method for Doppler-free spectroscopy was first suggested by Vasilenko et al. in [5]: two photons with opposite momentum get resonantly absorbed via a virtual state inside the atom, eliminating any contribution from its relative movement. Applying Doppler-free 2-photon ionization in-source in combination with the array of ion or radioisotope identification methods available at the ISOLDE facility, will enable high-resolution ( $< 100\text{ MHz}$ ) and high sensitivity ( $< 1\text{ ion/sec}$ ) studies, without limitation to the heavy mass range.

Under these conditions, the spectral resolution becomes limited by the laser linewidth. For a given laser power, the relatively low cross section of the 2-photon transition is mitigated by the gain in spectral brightness achieved by the desired reduction of the experimental laser linewidth.

Nevertheless, it is expected that achieving a high efficiency will require a transition for which the intermediate virtual state lies close in energy to a real state. This can be seen from the simplified form of the equation for the transition probability  $P_{gf}$  for a transition  $g \rightarrow f$  in the case of two photons of equal energy:

$$P_{gf} \propto \left( \sum_n \frac{\langle f|H|n\rangle \langle n|H|g\rangle}{\Delta\omega_n} \right)^2 \times \frac{1}{\Gamma_f}, \quad (1)$$

where  $H$  is the Hamiltonian of the electric dipole interaction between the photon and the atom,  $\Delta\omega_n$  is the wavelength difference from the virtual to a real single photon transition and  $\Gamma_f$  is the natural linewidth of the excited state  $f$ . In a more detailed description, given in [6], the complete formula for the transition probability is given, alongside the added components

\*corresponding author

Email address: kchrysal@cern.ch (K. Chrysalidis)

<sup>1</sup>CERN, CH-1211 Geneva, Switzerland

<sup>2</sup>Institut für Physik, Johannes Gutenberg-Universität, D-55099 Mainz, Germany

<sup>3</sup>KU Leuven, Instituut voor Kern- en Stralingsfysica, 3001 Leuven, Belgium

<sup>4</sup>Department of Physics, University of Jyväskylä, P. O. Box 35(YFL), FI-40014 Jyväskylä, Finland

<sup>5</sup>School of Physics and Astronomy, The University of Manchester, Manchester M13 9PL, United Kingdom

for the case of absorption of two photons with the same propagation vector. As will be seen in the spectra in section 2, this gives rise to a Doppler broadened background, upon which the Doppler-free peak is superimposed. Additionally, in the experiments presented here, this background is shifted: the atom source, transfer line and ion source geometry results in an atomic sample with predominantly forward-directed velocity components (towards the extraction electrode). In the rest-frame of an atom traveling towards the exit of the ion source, the light entering the source is blue-shifted, whereas the reflected light, from the rear of the ion source is red-shifted. The shift is in the order of the temperature induced Doppler broadening and overall, in case of equal intensities of the in- and out-going light, there will be no shift evident in the overall Doppler-broadened laser spectrum obtained. If, however, the reflectivity is less than 100 %, the Doppler-broadened spectrum will be dominated by the signal associated with the incoming (blue-shifted) light. As a result, the center of gravity (CoG) of the spectrum will be shifted to the lower frequency side (see Figure 1) of the Doppler-free center of the transition. Due to the nature and size of the Doppler broadening, it is impossible to disentangle the two different shifts from one another.

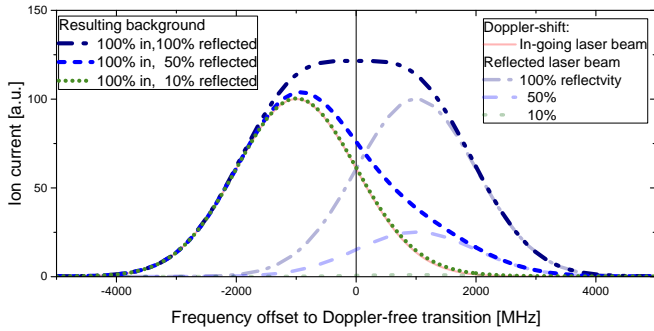


Figure 1: Simulated Doppler broadened and -shifted background. In case of equal light intensities, the center of gravity (CoG) is not shifted. The lower the reflectivity and therefore the intensity of the out-going light, the more the CoG is shifted towards lower frequencies. Additionally, the overall broadening is reduced and the asymmetry increased as the impact of the high frequency shift component reduces.

The feasibility of Doppler-free 2-photon resonance ionization spectroscopy inside a hot cavity environment has been demonstrated at Mainz University, where stable silicon isotopes were studied inside an atomic beam unit [7]. For this experiment, an open tube was used as the hot cavity, with a mirror placed outside of the vacuum chamber for reflecting the light for collinear laser beam propagation. This method is not suited for foreseen applications at ISOLDE, as the ion source and target areas are not accessible during on-line operation. Additionally, glass windows or mirrors would not survive the high radiation level. In this work we present results of experimental development performed both at Mainz University and CERN, which enabled Doppler-free measurements of rubidium 2-photon resonances inside a real ion source/target configuration of the CERN-ISOLDE facility.

## 2. Experimental setup and results

Spectroscopy was performed on  $^{87}\text{Rb}$ . The 2-photon transition excites atoms from the  $5S_{1/2}$  ground state to the  $5D_{1/2}$  state. The transition, along with the HFS splitting is depicted in Figure 2. Rubidium has been extensively studied and therefore comprehensive data is available for comparison of the spectra. However, the goal of this work was not an absolute measurement of the transition energies, but rather a measurement of the Doppler-free linewidth, in order to determine the feasibility of laser linewidth limited high-resolution in-source spectroscopy. In this work, HFS parameter as given in [8] were used for deriving the expected spectra for comparison with the data. Nevertheless, they were not used for fitting the measured spectra, since this went beyond the scope of the work presented here. At 2000 K the Doppler broadening is  $\sim 2.2$  GHz for stable rubidium isotopes. The frequency of the spectra is given relative to the transition centroid at  $25703.498\text{ cm}^{-1}$ .

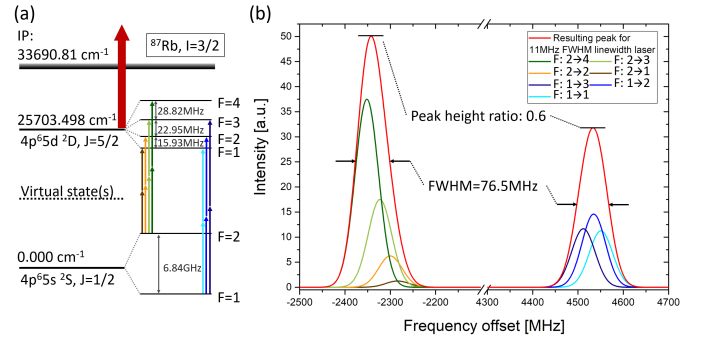


Figure 2: (a) Laser ionization scheme for rubidium. The hyperfine structure is depicted along with the corresponding shifts (not to scale) and the possible 2-photon transitions. (b) Simulated spectrum of the 2-photon HFS transitions with an assumed laser linewidth of 11 MHz (corresponding to 20 MHz minimal achievable transition linewidth). The individual transitions are included, but can not be resolved under the experimental conditions. All data used for the simulated spectrum has been taken from [8].

### 2.1. Experiments performed at the RISIKO mass separator in Mainz

The Laser Ion Source and Trap (LIST) was used for this test since it offers the ability to suppress surface-ionized contaminants, as has been shown previously in [9]. A molybdenum cylinder (2.8 mm diameter, 6 mm length) with polished top surface was inserted into the end of the hot cavity and used for reflecting the laser beam back into the ion source, as shown in Figure 3. In a separate test, the reflectivity of Mo was measured to be close to 50 % from 250 – 800 nm at up to 1600°C. The newest LIST design [10] also includes the possibility of perpendicular illumination of the atomic beam by displacing the laser beam and directing it towards stainless steel substrates covered with a gold layer by pulsed laser deposition. The two different geometries for the laser ionization are depicted schematically in Figure 3. As rubidium is easily surface ionized (IP = 4.18 eV [11]) it was necessary to operate the LIST in surface-ion-suppression mode by applying a positive voltage to

a repeller electrode located behind the hot cavity (offering 4–5 orders of magnitude suppression).

The laser system used for the tests comprises wavelength stabilized continuous wave (CW) diodes, fiber coupled to a seeded Ti:sapphire ring laser cavity, which was pumped by a 10 kHz Nd:YAG laser operating at 532 nm (see [7]). The Ti:sapphire cavity is based on the design by T. Kessler [12] and has been further developed by V. Sonnenschein [13]. An output power of up to 1.4 W was generated at a wavelength of 778.1 nm.

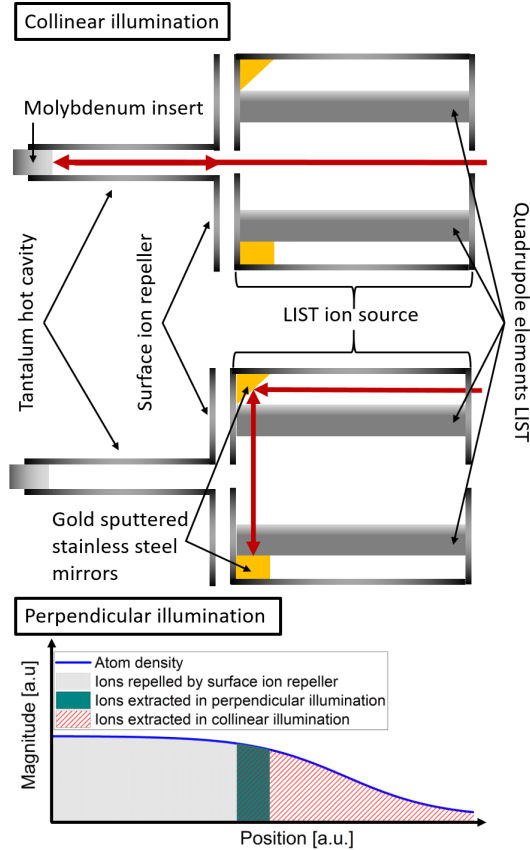


Figure 3: Schematic depiction of the two possible operating modes of laser ionization with the LIST. In collinear mode the laser beam is reflected by the polished surface of the molybdenum insert placed at the end of the ion source. In perpendicular mode the laser beam is entering the LIST off-axis and reflected on gold plated stainless steel mirrors. For both modes suppression of ions originating inside the hot cavity is achieved by applying a positive voltage to a repeller electrode located behind the hot cavity. The ionization probability (lower plot) is the same for collinear and perpendicular illumination, but the number of atoms with which the photons interact is higher for collinear illumination (see [14] for more details).

### Collinear illumination

In order to minimize saturation broadening of the spectral lines, the power was gradually reduced until the measured linewidth did not reduce further. The corresponding power was measured to be  $1.3 \mu\text{W}$ . In accordance with Equation 1, the saturation power required for the Rb 2-photon transition is lower than that required in a transition with a bigger separation of real and virtual state(s). Although saturation was reached with powers in the  $\mu\text{W}$ -range, this is not expected to be the case for most

applications of this technique. As will be shown later on (see subsection 2.2), higher powers are required e.g. if the mirror reflectivity is low.

The full spectral range spanning the splitting of the ground-state was scanned but is not shown in the spectrum, as no additional structures were observed. As was explained in section 1, the asymmetry of the Doppler-background stems from the non-equal intensities for photons absorbed from the co- and counter-propagating laser beams. Since the laser beams are focused to the ion-source diameter over a distance of  $> 3 \text{ m}$ , it can be assumed that the in-going and reflected laser beam have similar size. Therefore, no contribution to the asymmetry from the laser beam size is expected. The relatively large shift shows that the reflectivity of the molybdenum is low (estimated to be  $\ll 50\%$ ).

The extracted FWHM for the quadruplet and the triplet were

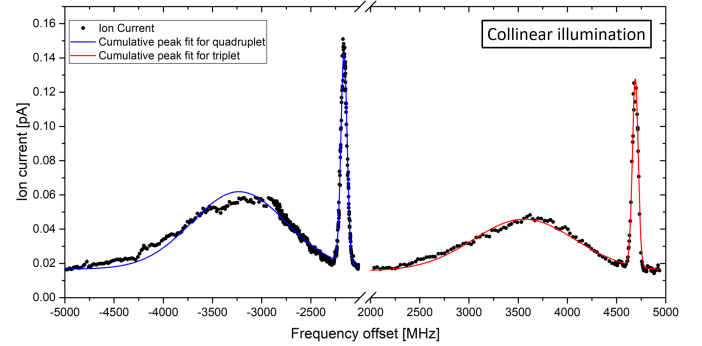


Figure 4: Spectrum for collinear illumination of the atomic beam. The Doppler-free 2-photon excitation peaks dominate the spectrum and are flanked by a Doppler broadened and shifted background.

determined to be  $85.7 \pm 0.4 \text{ MHz}$  and  $81.2 \pm 1.0 \text{ MHz}$ , respectively. Taking into account the distance of the outer peaks of the multiplets and the additional linewidth broadening effects due to the absorption of two photons, the upper linewidth limit for the laser was determined to be  $\leq 12.5 \text{ MHz}$  (compared to the Fourier-limited linewidth of  $\sim 10 \text{ MHz}$ ). It was extracted by varying the assumed laser linewidth (see Figure 2). The ratio of the peak heights was determined to be 0.84. This deviates from the expected ratio of 0.6 determined through angular-momentum coupling considerations (see [8]), but could be attributed to either saturation effects or ion source temperature fluctuations and resulting fluctuations in atom density at the ionization region. The ratio of Doppler-free signal to Doppler broadened background is 2.6 for the quadruplet and 2.7 for the triplet.

### Perpendicular illumination

For perpendicular illumination the laser beam was directed through an off-center hole inside the extraction electrode. In this case the laser is incident upon a  $45^\circ$  tilted gold plated stainless steel mirror surface, positioned near the hot cavity exit, adjacent to the LIST RFQ rods (see Figure 3). The mirrors used for perpendicular illumination of the atom cloud emerging from the hot cavity are located in the shadow of the LIST repeller, shielded from radiative heating by the hot cavity.

The obtained spectrum, shown in Figure 5, was taken with a laser power of 240 mW after the launch mirror and not optimized for saturation broadening suppression. Perpendicular illumination results in a reduced Doppler-broadening of the atomic line [15]. With perfect perpendicular alignment of the laser in respect to an ideal collimated atom beam, no asymmetry would be seen. Indeed this explains the lower separation distance of the Doppler broadened components of the spectrum to the Doppler-free components. The observed asymmetry in the presented spectrum is a result of the atom beam divergence and the angle of incidence of the laser beam.

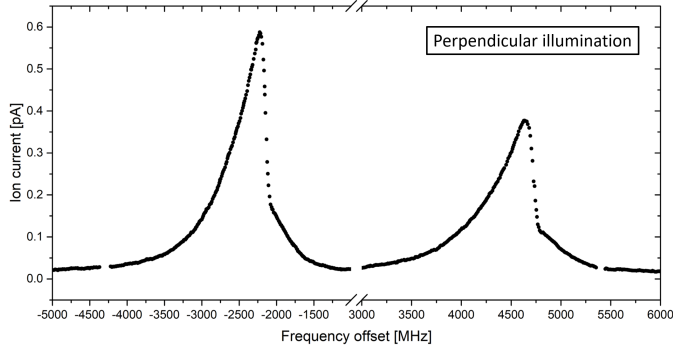


Figure 5: Spectrum for perpendicular illumination of the atom beam. The Doppler-free 2-photon absorption peaks are completely entangled with the Doppler broadened and -shifted background. Overall the achievable resolution is reduced due to the background becoming inseparable from the signal.

## 2.2. Experiments performed at the CERN-ISOLDE facility

A schematic overview over the pump and tunable lasers in RILIS, together with their according linewidth capabilities, is depicted in Figure 6. The ISOLDE RILIS is optimized for efficient ion beam production. The optimal laser linewidth is one which enables excitation of all atoms of interest in the interaction volume. Therefore, the lasers of the RILIS installation possess linewidths exceeding 800 MHz. For this work, to satisfy the laser linewidth requirements ( $< 100$  MHz) a new seeded Ti:sapphire ring laser, pumped by a 10 kHz doubled Nd:YAG at 532 nm, was constructed on a breadboard. It is a miniaturized cavity based on the design from [12] and the layout of this bow-tie cavity is shown in Figure 6. More details on this laser will be published in [16].

The CW light at 778 nm for seeding the Ti:sapphire cavity was generated by a commercial CW ring Ti:sapphire laser (Matisse 2 TS, Sirah-Lasertechnik GmbH) installed in the CRIS laser laboratory [17]. The seed light was transported via a 50 m long single-mode (SM) optical fiber, connecting the RILIS with the main laser laboratory of the CRIS collaboration. The total output power of the Matisse was 2 W, of which 100 mW were used for coupling into the fiber. After a first short (1 m) SM fiber, 70 mW were measured. With a commercial mating sleeve for SM fibers, this was then attached to the 50 m long fiber, where 25 mW emerged in RILIS. Measures, taken to avoid burning of the fiber by reverse direction light from the ring cavity (optical

Faraday insulator), further attenuated the CW light transmission to the laser to  $\sim 10$  mW. A second fiber connecting the two laser laboratories was used to measure the wavelength of the seeding CW laser simultaneously with that of the pulsed light emitted by the ring cavity using a HighFinesse/Angstrom WS7 wavelength meter installed in the RILIS laboratory. The wavemeter was calibrated before the measurements with a CW diode laser locked to the rubidium hyperfine structure (1-photon transition).

This experiment was performed in March 2018 using a ded-

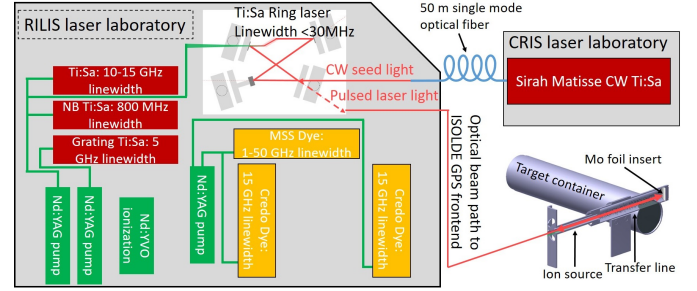


Figure 6: Schematic layout of laser setup used for 2-photon spectroscopy at ISOLDE. The RILIS lasers along with their linewidth capabilities are shown. The newly installed seeded Ti:sapphire ring cavity is pumped by a 10 kHz repetition rate Nd:YAG pump laser at 532 nm. The seed light is provided via a 50 m long single mode optical fiber. It transports laser light at  $\sim 778$  nm from the CRIS to the RILIS laser laboratory. The resulting pulsed light was transported via the optical beam path leading through the GPS mass separator, into the ISOLDE target/ion source assembly. It was reflected on a molybdenum foil at the end of the transfer line, for bi-directional illumination of the atomic vapor.

icated ISOLDE target and ion source development assembly (#594, Ta ion source) with a flat molybdenum foil inserted into the back of the transfer line. This unit had been used in the year 2017 for laser ionization scheme development of selenium [18]. A Rb dispenser was connected to the target/ion source assembly. These dispensers can be individually resistively heated to release an atomic vapor of the element of interest. The GPS front end and mass separator (General Purpose Separator with one  $60^\circ$  bending magnet) were used for the tests, and the ion beam current was recorded using a Faraday cup (GPS.FC490), situated behind the mass separation magnet. A sufficient suppression of rubidium surface ionization was achieved by reducing the heating currents of target and ion source cavity to 200 A and 50 A, respectively, corresponding to temperatures of  $< 850^\circ\text{C}$  and  $< 400^\circ\text{C}$ . The values cannot be given more precisely as the temperature calibration for target and ion source were performed under different conditions.

The laser beam positions were optimized to maximize the Doppler-free signal. This corresponds to the best possible overlap of the counter-propagating laser beams, so that finally the height ratio between narrow Doppler-free signal and Doppler broadened and -shifted background of 1.3 for the quadruplet and 1.4 for the triplet were reached, as can be seen in Figure 7. The FWHM of the Doppler-free resonance, measured at a laser power of 2 W before the laser beam delivery system to the ion source, was extracted to be  $126.7 \pm 2.2$  MHz for the triplet and  $138.0 \pm 2.4$  MHz for the quadruplet. Taking into account the high laser power compared to the below-saturation measure-

ments in Mainz, power broadening is assumed to be the main reason for the higher experimental linewidth. Additionally, the shorter resonator length leads to a shorter pulse length, increasing the Fourier-limited linewidth of the ring laser to  $\sim 12$  MHz. Judging by the reduced Doppler-free to Doppler broadened signal height ratio, we conclude that the mirror reflectivity in this case was lower than was the case for the RISIKO measurements (see Figure 4). As the target had been used prior to the experiment in 2018, a number of explanations for poor reflectivity of the foil are plausible:

- Depositions on the foil.
- Ablation of the molybdenum foil: a high power laser, which has been shown to cause ablation of the molybdenum foil during on-line experiments in 2018, had been used extensively with target #594. It is therefore assumed that the central part of the foil was damaged.
- Deformation or repositioning of the foil after repeated heating and cooling cycles of the target, or during target handling.

### 3. Outlook

In this first demonstration of in-source Doppler-free 2-photon spectroscopy at ISOLDE, the new seeded Ti:sapphire ring cavity has been shown to perform as required. A Doppler-free signal was successfully recorded. However, the signal height ratios indicate that there is room for significant improvement through an increase in mirror reflectivity. To this end, an alternative approach will be attempted. The mirror will be combined with the anode grid of the VADIS. An optimized environment for resonance laser ionization can be provided in the new VAD(L)IS design, suppressing surface ionization and enhancing extraction of laser-ionized species [19]. The possibility to install a perforated molybdenum mirror at the junction of the transfer line with the hot cavity is an alternative to this which is also being explored.

Systematic investigations into laser linewidth dependency of efficiency and saturation effects will be performed alongside

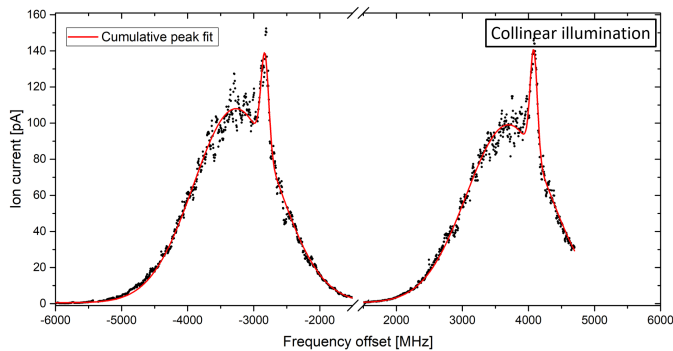


Figure 7: Measured spectral profiles of the 2-photon resonance excitation of rubidium atoms inside the ISOLDE RILIS hot cavity. The Doppler-free 2-photon absorption peaks have linewidths of  $126.7 \pm 2.2$  MHz for the triplet and  $138.0 \pm 2.4$  MHz for the quadruplet.

studies of the impact of close-lying real intermediate steps to the signal-to-background ratio. This method opens perspectives to development of resonance ionization schemes for elements with first step transitions requiring laser light at extremely short wavelengths, not easily achievable at RILIS. Schemes based on 2-photon transitions can be developed to overcome this limitation, enabling resonance laser ionization for elements that have so far been inaccessible. There are several examples, e.g. P, Kr, C and many more. Some feasible 2-photon transitions from the ground state can be found in the reviews ‘A resonance ionization spectroscopy/resonance ionization mass spectrometry data service. I-V’ by E. Saloman [20, 21, 22, 23, 24], giving a starting point for such developments.

### 4. Acknowledgments

This project has received funding from the European Union’s Horizon 2020 research and innovation program under grant agreement No 654002 and Bundesministerium für Bildung und Forschung (BMBF, Germany) under grant No 05P15UMCIA. Support was provided by collaborators from KU Leuven and the University of Manchester.

### References

- [1] V. Fedosseev, et al., J. Phys. G 44 (2017) 084006. Doi: .
- [2] B. A. Marsh, et al., Nature Physics 14 (2018) 1745–2473.
- [3] T. D. Goodacre, et al., NIM B 376 (2016) 39 – 45.
- [4] M. Göppert-Mayer, Annalen der Physik 401 (1931) 273–294.
- [5] L. Vasilenko, et al., JETP Letters 12 (1970) 113.
- [6] N. Bloembergen, M. D. Levenson (1976) 315–369.
- [7] K. Wendt, et al., Phys. Rev. A 88 (2013) 1–8.
- [8] F. Nez, et al., Optics Communications 102 (1993) 432 – 438.
- [9] D. Fink, et al., NIM B 344 (2015) 83 – 95.
- [10] R. Heinke, et al., Hyperfine Interactions 238 (2016) 6.
- [11] NIST Atomic Spectra Database (extracted 08.10.2018).
- [12] T. Kessler, et al., Laser Physics 18 (2008) 842.
- [13] V. Sonnenschein, et al., Characterization of a pulsed injection-locked Ti:sapphire laser and its application to high resolution resonance ionization spectroscopy of copper, Laser Phys. (2017).
- [14] R. Heinke, et al., NIM B (2019). In this issue.
- [15] D. N. Stacey, K. Burnett, Science Progress (1933- ) 73 (1989) 351–387.
- [16] K. Chrysalidis, M. Reponen, et al., Technical review of Ti:sapphire laser development within the scope of JRA RESIST, In preparation (2019).
- [17] A. Koszorus, et al., NIM B (2019). In this issue.
- [18] K. Chrysalidis, et al., Developments towards the delivery of selenium ion beams at ISOLDE (2019). In preparation.
- [19] Y. M. Palenzuela, et al., NIM B 431 (2018) 59 – 66.
- [20] E. Saloman, Spectrochim. Act. B (1990).
- [21] E. Saloman, Spectrochim. Act. B (1991).
- [22] E. Saloman, Spectrochim. Act. B (1992).
- [23] E. Saloman, Spectrochim. Act. B (1993).
- [24] E. Saloman, Spectrochim. Act. B (1994).